HHS Public Access

Author manuscript

J Neurosci Res. Author manuscript; available in PMC 2018 June 01.

Published in final edited form as:

J Neurosci Res. 2017 December ; 95(12): 2336–2344. doi:10.1002/jnr.24011.

Axonal sprouting in commissurally projecting parvalbumin-expressing interneurons

Zoé Christenson Wick, **Caara H. Leintz**, **Casey Xamonthiene**, **Bin H. Huang**, and **Esther Krook-Magnuson**

Neuroscience Department – University of Minnesota

Abstract

Previous research has shown that *in vivo* on-demand optogenetic stimulation of inhibitory interneurons expressing parvalbumin (PV) is sufficient to suppress seizures in a mouse model of temporal lobe epilepsy (TLE; Krook-Magnuson et al., 2013). Surprisingly, this intervention was capable of suppressing seizures when PV-expressing interneurons were stimulated ipsilateral or contralateral to the presumed seizure focus, raising the possibility of commissural inhibition in TLE. There are mixed reports regarding commissural PV interneuron projections in the healthy hippocampus, and it was previously unknown whether these connections would be maintained or modified following the network reorganization associated with TLE. Using retrograde labeling and viral vector technology in both sexes and the intrahippocampal kainate mouse model of TLE, we therefore examined these issues. Our results reveal that healthy controls possess a population of commissurally projecting hippocampal PV interneurons. Two weeks post-kainate injection, we see a slight, but not statistically significant decrease in retrogradely labeled PV interneurons in the hippocampus contralateral to kainate and tracer injection. By 6 months post-kainate, however, there is a significant increase in retrogradely labeled PV interneurons, suggesting commissural inhibitory axonal sprouting. Using viral GFP expression selectively in PV neurons, we demonstrate sprouting of commissural PV projections in the dentate gyrus of the kainate-injected hippocampus 6 months post-kainate. These findings indicate that PV interneurons supply direct inhibition to the contralateral hippocampus, and undergo sprouting in a mouse model of TLE.

Graphical Abstract

Corresponding author: Esther Krook-Magnuson; ekrookma@umn.edu; 6-145 Jackson Hall, 321 Church St SE, Minneapolis MN 55455.

Conflict of Interest: The authors declare that the research was conducted in the absence of any commercial or financial relationships that could be construed as a potential conflict of interest.

Role of authors: All authors had full access to the data in the study and take responsibility for the integrity of the data and the accuracy of the data analysis. Study concept and design: EK-M, ZCW. Acquisition of data: ZCW, CHL, CX, BHH. Analysis and interpretation of data: EK-M, ZCW. Statistical analysis: EK-M, ZCW. Drafting of the manuscript: ZCW, CHL, BHH, CX, EK-M. Study supervision: EK-M.

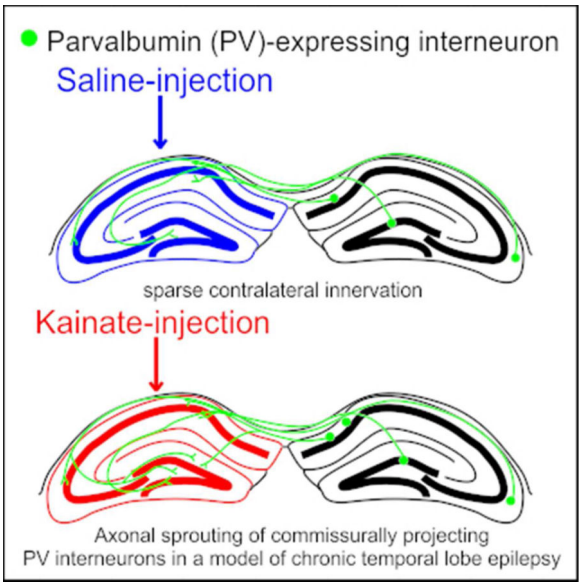

Parvalbumin-expressing interneurons sparsely innervate the contralateral hippocampus in saline-injected control mice. 6 months following intrahippocampal kainate injection (to model temporal lobe epilepsy), axonal sprouting of commissurally projecting parvalbumin-expressing interneurons occurs, primarily targeting the dentate gyrus. This illustrates long-range reorganization of the inhibitory hippocampal network in temporal lobe epilepsy.

Keywords

axonal sprouting; inhibitory interneuron; parvalbumin; commissural; epilepsy; Fluorogold; hippocampus; RRID: AB_2631173

INTRODUCTION

Temporal lobe epilepsy (TLE) is the most common form of partial epilepsy in adults. In TLE, spontaneous seizures originate from areas within the temporal lobe, often the hippocampus. Unfortunately, for many individuals with TLE, currently available anti-epileptic medications are ineffective. Further understanding of the disorder and the associated network reorganization may uncover new targets for more effective therapies. It was previously shown that *in vivo* on-demand optogenetic excitation of parvalbumin (PV)-expressing GABAergic interneurons suppresses spontaneous seizures in the intrahippocampal kainate (IHKA) mouse model of TLE (Krook-Magnuson et al., 2013). Surprisingly, this remained true irrespective of whether PV interneurons were excited ipsilaterally or contralaterally to the kainate (KA) injected hippocampus and presumed seizure focus. While it is well-established that PV interneurons powerfully affect principal cell activity ipsilaterally (Cobb et al., 1995; Hajos and Paulsen, 2009; Sohal et al., 2009), it is unclear how PV interneuron activity might suppress contralateral seizures. One possible explanation for PV interneuron-mediated contralateral seizure suppression is that the powerful inhibition which PV interneurons supply to excitatory cells at the local level is sufficient to suppress seizures in the contralateral hippocampus. This explanation is

unsupported, however, because direct optogenetic inhibition of granule cells contralateral to the site of KA injection is not sufficient to suppress seizures (Krook-Magnuson et al., 2015). While this does not rule out the possibility of PV interneurons inhibiting seizures through local inhibition to commissurally projecting CA3 pyramidal cells and mossy cells, there may be an alternative mechanism at play.

One such possibility is that there may exist long-range, commissural, projections from PV interneurons which directly inhibit the KA injected hippocampus. Some interneurons are known to have long-range projections connecting the hippocampus to extra-hippocampal areas, including the medial septum (Freund and Antal, 1988; Takács et al., 2008) and the medial entorhinal cortex (Melzer et al., 2012). However, there exist discrepancies in the literature regarding the extent to which hippocampal PV interneurons project contralaterally (Goodman and Sloviter, 1992; Zappone and Sloviter, 2001; Ratzliff et al., 2004; Sun et al., 2014). Furthermore, it was unknown whether such commissural projections from PV neurons would be preserved or modified during the network reorganization associated with TLE. Studies analyzing epileptic tissue show that there can be massive reorganization of the hippocampal network including cell death, granule cell dispersion, and axonal sprouting (Babb et al., 1984; Houser, 1990; Sutula et al., 1989; Santhakumar et al., 2005; Ang et al., 2006; Scharfman and Pierce, 2012; Hester and Danzer, 2014).

While axonal sprouting in epilepsy is typically associated with excitatory cells (e.g., mossy fiber sprouting; Laurberg and Zimmer, 1981; Tauck and Nadler, 1985; Sutula et al., 1989; Buckmaster and Dudek, 1997; Althaus et al., 2016), there are also reports of inhibitory axonal sprouting (Zhang et al., 2009; Peng et al., 2013; Soussi et al., 2015). In this vein, we set out to answer the following questions: 1) do PV interneurons have commissural projections in healthy mice? 2) do PV interneurons have commissural projections following IHKA injection? and 3) if these commissural projections exist, which subfields of the contralateral hippocampus do they target? In addressing these questions, we found a small percentage of PV interneurons labeled with retrograde tracer in saline injected controls. By 6 months post-KA, the number of retrogradely labeled PV interneurons had significantly increased, suggesting long-range axonal sprouting. Using viral expression of GFP in PV neurons, we found commissural fibers in CA subfields and the dentate gyrus (DG). Complementing the retrograde tracing experiments, 6 months post-KA injection there was a significant increase in GFP fibers in the dentate (more than 100× increase), indicating axonal sprouting of commissural axons from PV interneurons.

MATERIALS & METHODS

All experimental protocols were approved by the Institutional Animal Care and Use Committee of the University of Minnesota.

Animals

For Fluorogold experiments, C57BL/6J mice were obtained from Jackson Laboratories (stock 000664). For AAV experiments, mice expressing Cre in PV-containing interneurons, including bistratified cells, fast-spiking basket cells, and chandelier cells (Freund and Buzsáki, 1996), were bred in-house after obtaining founders from Jackson labs (PV-Cre;

B6;129P2-Pvalbtm1(cre)Arbr/J; stock 008069; Hippenmeyer et al., 2005). Both male and female mice were used. Animals were housed in standard housing conditions with 12-hour light, 12-hour dark cycles in the animal facility at the University of Minnesota.

Stereotaxic Surgeries

Surgical procedures were performed stereotaxically under isoflurane anesthesia and 0.5% bupivacaine to induce local nerve block (as in Krook-Magnuson et al., 2013; Armstrong et al., 2013).

Intrahippocampal Kainate & Saline Injections—Kainic acid (KA; 100nL, 20mM in saline; Fisher Scientific, stock 22210) was injected using a Hamilton syringe into the left dorsal hippocampus (2.0mm posterior, 1.25mm left, and 1.6mm ventral to bregma; similar to Krook-Magnuson et al., 2013) of mice after postnatal day 46. Saline (100nL) was injected in the same manner in littermate controls. Animals were removed from isoflurane anesthesia less than 10 minutes after injection of kainate or saline (as done previously in Krook-Magnuson et al., 2013, 2014, 2015). After recovery, animals were returned to the animal housing facility until subsequent Fluorogold or virus injections.

Fluorogold Injections—C57BL/6J mice were then injected with the fluorescent retrograde tracer Fluorogold (FG; 100nL, 4% in saline; Fluorochrome, LLC) into the left dorsal hippocampus (2.6mm posterior, 1.75mm left, and 2.0mm ventral to bregma) 2 weeks, 1 month, 4 months, or 6 months after the date of KA or saline injection. We positioned the FG injection in this location to match the light delivery in Krook-Magnuson et al., 2013. To examine the acute extent of FG injection, the brain of one mouse was acutely dissected and visualized for each day of FG injections. The brains of all other FG-injected mice were dissected at least 1 week following FG injection to permit retrograde transport of FG.

Virus Delivery—4.5 months following KA or saline injection, PVCre mice were injected with 2μl of a virus which would lead to expression of green fluorescent protein (GFP) in a Cre-dependent manner (AAV8-CAGFLEX-GFP, UNC Vector Core, 6.2×10^{12} virus molecules/mL) into the right dorsal hippocampus (2.6mm posterior, 1.75mm right, and 2.0mm ventral to bregma). Following recovery, animals were housed for 6 weeks to achieve strong axonal expression. Brains were dissected and processed for PV immunohistochemistry 6 months following KA or saline injection.

Antibody Characterization

See Table I for a description of the antibody used. The manufacturer (Swant) found that the PV27 antiserum labeled only the expected subpopulation of neurons in the normal mouse brain with high efficiency, and did not stain any neurons in the brain of PV knock-out mice. In our sections, PV immunofluorescence labeling matched the expected pattern of PV expression (Freund and Buzsáki, 1996).

Immunohistochemistry

Brains were fixed in 0.1M phosphate buffer containing 4% paraformaldehyde and 0.1% picric acid. Using a vibratome (Leica VT1000S), 50μm coronal (for FG animals) or sagittal

(for virus animals) brain sections were then collected in 0.1M phosphate buffer at room temperature. To locate PV-expressing cells, sections were incubated with the polyclonal rabbit anti-PV primary antibody (Swant, Cat# PV27, RRID: AB_2631173, Table I) at a 1:1000 dilution ratio overnight in Tris-buffered saline containing 0.5% Triton X-100 at 4°C, followed by Alexa Fluor 594-conjugated secondary goat antibody against rabbit (Jackson ImmunoResearch) at a 1:500 dilution ratio incubated for 2 hours at room temperature. Sections with FG and PV immunofluorescence were mounted with Vectashield mounting media for fluorescence without DAPI. Sections with GFP and PV immunofluorescence were mounted with Vectashield mounting media with DAPI.

Imaging, Cell Counting, & Neurite Tracing

Sections with FG and PV immunofluorescence were viewed and imaged on a Zeiss Axioplan 2 Upright Microscope in the University of Minnesota Imaging Center. In every 4th section, all subfields of the right hippocampus (contralateral to site of KA, saline, and FG injections) spanning from 1.6mm to 3mm posterior to bregma were imaged for PV and FG fluorescence (8 sections per animal). All PV-immunoreactive (PV+) cells in the hippocampus (defined here as all CA subfields and the DG; cells in the subiculum were not included in these analyses) in a single plane of focus per section were counted and examined for FG signal colocalization. This provided a total number of counted PV+ cells per animal and a percent of PV+ cells which were FG-positive for each animal. All statistical analysis was then done at the group (animal) level.

Sections with GFP and DAPI fluorescence and PV immunofluorescence were viewed on a Leica DM2500 microscope and imaged with an Olympus FluoView FV1000 BX2 upright confocal microscope. Every section was viewed to confirm the location of viral delivery, to verify GFP expression in PV+ cells, and to establish the location of GFP-labeled cell bodies and axons. GFP-labeled cells in one focal plane were counted at the virus injection site and checked for PV immunofluorescence, and all (100%) were found to be PV+. Two mice (1 KA-injected, 1 saline-injected) showed drastically lower transfection of the GFP virus and were therefore excluded from analysis.

Some axonal uptake of the virus occurred (in addition to dendritic/somatic infection) as illustrated by GFP-labeled cell bodies located in areas projecting to the hippocampus including the posterior subiculum, and septum. Perhaps due to the sparse nature of commissural PV+ fibers and cell loss ipsilateral to KA, GFP-labeled cell bodies were not found in the hippocampus contralateral to viral injection in most mice: all hippocampal subfields and the subiculum of every section contralateral to virus injection were examined for GFP-labeled cell bodies at 20×. GFP-labeled cell bodies were found in the KA/saline-injected hippocampus of two mice (1 KA-injected, 1 saline-injected), and those mice were therefore excluded from analysis. The left hippocampus (ipsilateral to KA/saline injection) was then viewed for GFP-labeled fibers to determine whether PV+ cells expressing the Cre-dependent GFP virus had processes in the left hippocampus (contralateral to viral injection) of healthy controls and mice 6 months following KA injection. Confocal images of GFP-labeled fibers in the left (KA/saline-injected) hippocampus (0.84mm left of the sagittal sinus) were taken and neurites within the CA subfields and DG were measured using Fiji's

Simple Neurite Tracer. Images in figures were adjusted for brightness and contrast, with all adjustments applied to the entire image.

Statistical Analysis

The percentage of PV+ cells co-labeled with FG at different time-points was compared between KA- and saline-injected animals using two-tailed Mann-Whitney tests with Bonferonni correction for multiple comparisons. Length of neurites measured in the DG was compared between KA- and saline-injected animals using a two-tailed Mann-Whitney test. Correlations between percent of PV+ cells co-labeled with FG and age or time since KA/saline injection were tested with Spearman's rho. Values are presented as mean ± standard error of the mean (SEM). A p-value of less than 0.05 was considered significant. Statistical analysis was done using OriginPro 2016.

RESULTS

PV+ cells project commissurally

To examine inhibitory commissural connections, we injected the retrograde tracer Fluorogold (FG) into the left dorsal hippocampus and investigated the cells retrogradely labeled with FG in the right hippocampus. In order to first ensure that the FG signal in the right hippocampus (contralateral to KA/saline/FG injection) was due entirely to retrograde labeling, one brain was dissected on each day of FG injections and examined for the acute extent of FG. At the acute time-point, FG was seen in the left hippocampus and along the injection tract running through the retrosplenial cortex (Fig. 1A). FG was also seen in the most dorsal aspect of the left thalamus in 4 of 9 mice. No FG invaded the right hippocampus of any animals at the acute time-point (Fig. 1A), indicating that any FG seen in the right hippocampus at later time-points was indeed due to retrograde labeling.

As a positive control, we examined the right hippocampus (contralateral to KA/saline/FG injection) 1 week following FG injection and confirmed that somata labeled with FG were located in areas known to provide commissural projections including the DG hilus (Fig. 1B, left panel) and CA3 pyramidal layer (Fig. 1B, right panel; Ribak et al., 1985, 1986; Goodman and Sloviter, 1992). In contrast and as expected, FG was absent from granule cells in the DG, a population of cells which do not have commissural projections (Fig. 1B, left panel). Taken together, the absence of observed FG in the right hippocampus immediately following FG injection, the absence of FG in granule cells, and FG-labeling in cells with known commissural projections suggest that the retrograde transport of FG occurred as expected and that FG seen in the right hippocampus (contralateral to KA/saline/FG injection) was a result of retrograde labeling.

To test whether hippocampal PV+ cells have commissural projections, immunofluorescent PV+ cells were counted in all subfields of the right hippocampus (contralateral to KA/saline/FG injections) and examined for co-labeling with FG. Across animals, PV+ cells co-labeled with FG were found in CA1, CA3, and the DG (Fig. 1D–F, Fig. 2). While present, they made up a very small fraction of the population of PV+ cells in saline-injected control mice (Fig. 1C; 0.51% ± 0.14 PV+ cells labeled with FG) and were most often seen in the

stratum oriens of CA1 (Fig. 2C). There was a negative correlation between percent of PV+ cells co-labeled with FG and time since saline injection (Spearman's $\rho = -0.58$, n = 24 animals, $p < 0.05$). However, this relationship was better explained by age; the correlation between percent of PV+ cells co-labeled with FG and the age of the mouse was greater (Spearman's $\rho = -0.75$, n = 24 animals, $p < 0.001$). These findings suggest that a population of hippocampal PV+ cells do in fact have commissurally projecting axons in saline-injected mice, though this may be very sparse in adult mice.

Commissural PV+ projections increase following IHKA

We next determined whether the population of commissurally projecting PV+ cells found in saline-injected mice was maintained following the network reorganization that accompanies IHKA injections acutely and chronically. As in saline-injected mice, PV+ cells co-labeled with FG were found in CA1, CA3, and the DG of the right hippocampus in KA-injected mice (Fig. 2B). However, in contrast to the negative correlation seen in saline mice, there was a strong positive correlation between percent of PV+ cells co-labeled with FG and time since KA injection (Spearman's $\rho = 0.79$, n = 22 animals, $p < 0.001$). This relationship was better explained by time since KA injection than by age (Spearman's $\rho = 0.59$, n = 22 animals, $p < 0.05$).

Two weeks following KA injection there was a modest, but not statistically significant, decrease in PV+ cells co-labeled with FG when compared to saline controls (Fig. 1C; 0.14% ± 0.07, n = 6 animals, vs 0.51% in saline controls as discussed above, uncorrected $p = 0.22$). However, 6 months post-KA, the percentage of FG labeled PV+ cells rebounded (1.67% ± 0.19, n = 5 animals), and was actually significantly increased (Fig. 1C; Mann-Whitney, vs. saline-injected controls, $p < 0.01$, corrected for multiple comparisons). This remained true whether the percentage of FG labeled PV+ cells was compared to all saline controls (n = 24) or to just 6 month saline controls (n = 7). Additionally, there were no apparent sex differences in percentage of FG labeled PV+ cells between male and female mice (Fig. 1C, inset). Importantly, in the right hippocampus (contralateral to KA/saline/FG injection), no change in the total number of PV+ interneurons was observed between saline- and KA-injected mice, nor was there any effect of time since injection on PV+ interneuron number ($p > 0.05$ for all comparisons, n = 24 saline, 23 KA animals). This suggests that the significant increase in FG-labeled PV+ cells seen at 6 months post-KA (Fig. 1C) may be caused by long-range axonal sprouting in the KA-injected hippocampus.

Sprouting of commissural PV+ cell projections into the DG following IHKA

To confirm that the co-labeling of PV+ cells with FG was a result of PV+ cell axons located within the left (KA/saline-injected) hippocampus and to determine which subfields are targeted by these commissurally projecting neurons, we injected the right hippocampus (contralateral to KA/saline-injected) with a virus to express GFP in a Cre-dependent manner in mice expressing Cre recombinase selectively in PV-containing cells and examined expression 6 months following KA/saline injection. In the right (virus-injected) hippocampus, we saw successful expression of the GFP virus in PV+ cells (Fig. 3B, 3C). There was no difference in the number of GFP-labeled cells between KA- and saline-injected mice (counted at virus injection site, $p = 0.33$, n = 5 saline, 4 KA animals). GFP-

labeled fibers were seen crossing the midline in the dorsal hippocampal commissure (data not shown), and GFP-labeled fibers were found in the left (KA/saline-injected) hippocampus in CA1, CA3, and the DG of both saline- and KA-injected mice (Fig. 3). This shows that commissurally projecting PV interneurons are capable of targeting several subfields of the contralateral hippocampus. While CA1, CA3, and the DG were all targeted in both saline and KA treated animals, the length of GFP-labeled neurites located within the DG specifically was drastically increased 6 months post-KA (by more than 100 times; Fig. 3A; vs. 6 months post-saline, $p < 0.05$, n = 5 saline, 4 KA animals). Taken together, our results indicate that PV+ cells can indeed project commissurally in healthy controls and that this innervation is not only maintained, but significantly increased 6 months following IHKA injection (Fig. 1C), with axonal sprouting primarily targeting the DG (Fig. 3A).

DISCUSSION

We demonstrate that PV+ interneurons have commissural projections that undergo plasticity in a mouse model of TLE. Specifically, following a modest, but non-significant, acute decrease in FG labeling of contralateral PV+ neurons, by 6 months post-KA injection, there was a significant increase in FG labeling of contralateral PV+ neurons. This increase in FG+ labeling 6 months after KA injection was paralleled by an increase in virally labeled fibers in the dentate ipsilateral to KA injection, indicating sprouting of PV+ interneurons' long-range commissural axons.

TLE is associated with significant network reorganization, including axonal sprouting. While this is typically considered in the context of excitatory connections (including mossy fiber sprouting; Laurberg and Zimmer, 1981; Tauck and Nadler, 1985; Sutula et al., 1989; Buckmaster and Dudek, 1997; Althaus et al., 2016), GABAergic sprouting has also been long suggested in the literature, including in human tissue (Babb et al., 1989; Davenport et al., 1990; Arellano et al., 2004; Bausch, 2005). Additionally, recent studies have clearly demonstrated inhibitory axonal sprouting. Using GIN mice, which express GFP in somatostatin-expressing interneurons, and the pilocarpine model of TLE, Buckmaster and colleagues demonstrated that surviving hilar somatostatin cells undergo extensive axonal sprouting (Zhang et al., 2009; Buckmaster and Wen, 2011). After an initial decrease in somatostatin fibers (visualized through GFP expression), there is a marked increase, resulting in over twice the GFP-positive axon length per DG compared to control animals (Buckmaster and Wen, 2011). An additional study by Houser and colleagues (Peng et al., 2013) found sprouting of somatostatin CA1 interneurons – axons from these CA1 interneurons invaded the DG, contributing to an increase in somatostatin labeling in the dentate observed at 1–3 months post-status epilepticus.

Similar to these previous studies reporting sprouting of inhibitory axons in temporal lobe epilepsy, we report that after a slight initial decrease, there is significant inhibitory axon sprouting months after the initial insult. Clearly, however, our findings illustrate axonal sprouting of parvalbumin (rather than somatostatin) expressing interneurons. More importantly, this sprouting is done by commissurally projecting interneurons, with an impressive distance between the inhibitory cells' somata and the area targeted by axonal sprouting. Also similar to the findings from Houser and colleagues, the sprouting we report

increases inhibition to the DG from outside sources (in our case, from the contralateral hippocampal formation) in epileptic animals. Previously, following transection of entorhinal input, increased branching of commissural inhibitory fibers to the dentate was reported using *Phaseolus vulgaris* leucoagglutinin (PHAL) anterograde tracing and GABA immunocytochemistry (Deller et al., 1995). Additionally, long-range axonal remodeling of supramammillary input to the dentate in a model of temporal lobe epilepsy was recently reported (Soussi et al., 2015), indicating that commissural inhibitory axonal sprouting may not be unique in regards to the distance at which axonal remodeling can occur.

GABAergic projection neurons, both projecting into the hippocampus and from the hippocampus to other areas, are well established (Jinno et al., 2007; Tóth et al., 1993; Ceranik et al., 1997; Takács et al., 2008; Melzer et al., 2012; Mattis et al., 2014; Lübkemann et al., 2015). Commissurally projecting GABAergic interneurons in particular have also been suggested for some time (Bakst et al., 1986; Ribak et al., 1986), with high percentages (up to 84% in some sections) of PV+ cells reported to have commissural projections in some studies (Goodman and Sloviter, 1992; Zappone and Sloviter, 2001). Other studies, like ours, have reported at most only scarce retrograde labeling of contralateral interneurons following hippocampal injections of tracers or rabies virus (Bakst et al., 1986; Ribak et al., 1986; Deller and Leranth, 1990; Ratzliff et al., 2004; Sun et al., 2014). This discrepancy may in part be due to differences in methods and inhibitory cell populations examined, including, importantly, the area targeted with initial tracer/virus. For example, in animals injected with FG into the dorsal hippocampus, Zappone and Sloviter report up to 26% of PV cells in the dorsal dentate being labeled with FG, but zero ventral dentate PV cells were found to be FG-labeled. Additionally, the number of FG-labeled cells was dependent on the size of the FG spread in the injected hippocampus (Zappone and Sloviter, 2001). In the same study, they report an absence of FG-labeled interneurons in the granule cell layer after ventral FG injections (Zappone and Sloviter, 2001). Therefore, the size and site of the FG injection may be a critical factor. However, while our study is in mouse instead of rat, the relative area of hippocampus injected in our current study appears to be fairly similar to the dorsal injections in Zappone and Sloviter (2001). Therefore, the injection location may not be the major contributor to the difference in percent of PV cells labeled in our study. Another possible explanation is the age related decline in FG labeled cells we find in control animals. Based on the reported weights of the animals, the rats used in the study by Zappone and Sloviter (2001) may have been relatively young (perhaps only a couple of months old). Future work can clarify the percentage of PV cells which have commissural projections in juvenile animals.

Our results suggest extremely limited connections in adult animals, with roughly one half of one percent of contralateral hippocampal PV+ cells displaying uptake of FG overall. However, despite an age-related decline in control animals, the percent of FG-labeled PV+ cells significantly *increases* 6 months after KA injection. This could indicate completely *de novo* commissural projections from interneurons which do not normally project contralaterally or sprouting of already present, but extremely sparse, fibers. In this latter scenario, the increase in contralateral fibers (and possible invasion of areas within the contralateral hippocampus not normally targeted by those fibers) would allow greater uptake of tracer, and a greater percentage of FG-labeled PV+ cells. Both scenarios are compatible

with our current findings of an increased percent of FG-labeled PV+ cells 6 months following KA injection, and either situation would result in increased inhibitory control over the contralateral hippocampus.

Given the increase in contralateral inhibitory input, the question becomes: is this beneficial? Increasing inhibition, even in the form of aberrant synapses, may be able to reduce over-excitability and curtail seizures. However, this inhibitory axon sprouting would also act to increase the coherence of the two hippocampi, and may introduce increased synchrony, with potential detrimental impacts on cognition and disease progression. Of interest, when sprouting of mossy fibers and somatostatin interneurons is experimentally blocked with rapamycin administration, there is no observable change in seizure frequency or severity (Buckmaster and Lew, 2011; Buckmaster and Wen, 2011). If axonal sprouting of commissurally projecting PV interneurons is similarly sensitive to rapamycin treatment, then the previous studies examining the effect of blocking sprouting would have also blocked sprouting from PV interneurons. This would suggest that - at least when combined with other axonal sprouting (including excitatory sprouting) - there is no net positive or negative outcome with regards to seizures of PV interneuron axonal sprouting. Of course, if only inhibitory sprouting were blocked, while excitatory axonal sprouting was maintained, a different picture might emerge. Importantly, however, regardless of the native effects of inhibitory axonal sprouting, recent studies indicate that interneurons can be harnessed to provide seizure control. Specifically, on-demand optogenetic excitation of contralateral hippocampal PV interneurons is able to significantly inhibit seizures (Krook-Magnuson et al., 2013). Reexamination of the time point post-KA for this prior work showed that contralateral light delivery to animals expressing channelrhodopsin in PV neurons occurred on average 6 months (SD: 2.6 months; median: 5.6 months) after kainate injection, and therefore at a time when sprouting would have occurred. While other potential mechanisms for the inhibition of seizures with contralateral excitation of PV neurons are certainly possible, our findings indicate that commissural projections are one possible mechanism. Further investigation into the potential of long-range inhibitory projections for future seizure control intervention strategies is warranted.

Acknowledgments

This work was supported by the University of Minnesota's MnDRIVE (Minnesota's Discovery, Research and Innovation Economy) initiative (to EK-M) and a National Institutes of Health grant (R00 NS087110, to EK-M). The authors would also like to thank Hannah Springer and Sean Lew for their contributions to the work as well as Zachary Zeidler and Alexandra Doyle for aiding in the editing of this paper.

LITERATURE CITED

Althaus AL, Zhang, Parent JM. Axonal plasticity of age-defined dentate granule cells in a rat model of mesial temporal lobe epilepsy. Neurobiol Dis. 2016; 86:187–196. [PubMed: 26644085]

Ang CW, Carlson GC, Coulter DA. Massive and specific dysregulation of direct cortical input to the hippocampus in temporal lobe epilepsy. J Neurosci. 2006; 26:11850–11856. [PubMed: 17108158]

Arellano J, Muñoz A, Ballesteros-Yáñez I, Sola R, DeFelipe J. Histopathology and reorganization of chandelier cells in the human epileptic sclerotic hippocampus. Brain. 2004; 127:45–64. [PubMed: 14534159]

Armstrong C, Krook-Magnuson E, Oijala M, Soltesz I. Closed-loop optogenetic intervention in mice. Nat Protoc. 2013; 8:1475–1493. [PubMed: 23845961]

Babb T, Brown W, Pretorius J, Davenport C, Lieb J, Crandall P. Temporal lobe volumetric cell densities in temporal lobe epilepsy. Epilepsia. 1984; 25:729–740. [PubMed: 6510381]

Babb T, Pretorius J, Kupfer W, Crandall P. Glutamate decarboxylase-immunoreactive neurons are preserved in human epileptic hippocampus. J Neurosci Official J Soc Neurosci. 1989; 9:2562–2574.

Bakst I, Avendano C, Morrison J, Amaral D. An experimental analysis of the origins of somatostatin-like immunoreactivity in the dentate gyrus of the rat. J Neurosci Official J Soc Neurosci. 1986; 6:1452–1462.

Bausch S. Axonal sprouting of GABAergic interneurons in temporal lobe epilepsy. Epilepsy & behavior E&B. 2005; 7:390–400.

Buckmaster PS, Dudek FE. Neuron loss, granule cell axon reorganization, and functional changes in the dentate gyrus of epileptic kainate-treated rats. J Comp Neurol. 1997; 385:385–404. [PubMed: 9300766]

Buckmaster PS, Lew FH. Rapamycin suppresses mossy fiber sprouting but not seizure frequency in a mouse model of temporal lobe epilepsy. J Neurosci. 2011; 31:2337–2347. [PubMed: 21307269]

Buckmaster PS, Wen X. Rapamycin suppresses axon sprouting by somatostatin interneurons in a mouse model of temporal lobe epilepsy. Epilepsia. 2011; 52:2057–2064. [PubMed: 21883182]

Ceranik K, Bender R, Geiger JR, Monyer H, Jonas P, Frotscher M, Lübke J. A novel type of GABAergic interneuron connecting the input and the output regions of the hippocampus. J Neurosci Official J Soc Neurosci. 1997; 17:5380–5394.

Cobb SR, Buhl EH, Halasy K, Paulsen O, Somogyi P. Synchronization of neuronal activity in hippocampus by individual GABAergic interneurons. Nature. 1995; 378:75–78. [PubMed: 7477292]

Davenport CJ, Brown WJ, Babb TL. Sprouting of GABAergic and mossy fiber axons in dentate gyrus following intrahippocampal kainate in the rat. Exp Neurol. 1990; 109:180–190. [PubMed: 1696207]

Deller T, Frotscher M, Nitsch R. Morphological evidence for the sprouting of inhibitory commissural fibers in response to the lesion of the excitatory entorhinal input to the rat dentate gyrus. J Neurosci. 1995; 15:6868–6878. [PubMed: 7472444]

Deller T, Leranth C. Synaptic connections of neuropeptide Y (NPY) immunoreactive neurons in the hilar area of the rat hippocampus. J Comp Neurol. 1990; 300:433–447. [PubMed: 2266195]

Freund TF, Antal M. GABA-containing neurons in the septum control inhibitory interneurons in the hippocampus. Nature. 1988; 336:170–173. [PubMed: 3185735]

Freund TF, Buzsáki G. Interneurons of the hippocampus. Hippocampus. 1996; 6:347–470. [PubMed: 8915675]

Goodman JH, Sloviter RS. Evidence for commissurally projecting parvalbumin-immunoreactive basket cells in the dentate gyrus of the rat. Hippocampus. 1992; 2:13–21. [PubMed: 1284972]

Hester MS, Danzer SC. Hippocampal granule cell pathology in epilepsy - a possible structural basis for comorbidities of epilepsy? Epilepsy Behav. 2014; 38:105–116. [PubMed: 24468242]

Hippenmeyer S, Vrieseling E, Sigrist M, Portmann T, Laengle C, Ladle D, Arber S. A developmental switch in the response of DRG neurons to ETS transcription factor signaling. PLoS biology. 2005; 3:e159. [PubMed: 15836427]

Houser C. Granule cell dispersion in the dentate gyrus of humans with temporal lobe epilepsy. Brain Res. 1990; 535:195–204. [PubMed: 1705855]

Hájos N, Paulsen O. Network mechanisms of gamma oscillations in the CA3 region of the hippocampus. Neural Netw. 2009; 22:1113–1119. [PubMed: 19683412]

Jinno S, Klausberger T, Marton L, Dalezios Y, Roberts D, Fuentealba P, Bushong E, Henze D, Buzsaki G, Somogyi P. Neuronal Diversity in GABAergic Long-Range Projections from the Hippocampus. J Neurosci. 2007; 27:8790–8804. [PubMed: 17699661]

Krook-Magnuson E, Armstrong C, Bui A, Lew S, Oijala M, Soltesz I. In vivo evaluation of the dentate gate theory in epilepsy. J Physiol (Lond). 2015; 593:2379–2388. [PubMed: 25752305]

Krook-Magnuson E, Armstrong C, Oijala M, Soltesz I. On-demand optogenetic control of spontaneous seizures in temporal lobe epilepsy. Nat Commun. 2013; 4:1376. [PubMed: 23340416]

Krook-Magnuson E, Szabo GG, Armstrong C, Oijala M, Soltesz I. Cerebellar Directed Optogenetic Intervention Inhibits Spontaneous Hippocampal Seizures in a Mouse Model of Temporal Lobe Epilepsy. eNeuro. 2014; 1

Laurberg S, Zimmer J. Lesion-induced sprouting of hippocampal mossy fiber collaterals to the fascia dentata in developing and adult rats. J Comp Neurol. 1981; 200:433–459. [PubMed: 7276246]

Lübkemann R, Eberhardt J, Röhl F-WW, Janitzky K, Nullmeier S, Stork O, Schwegler H, Linke R. Identification and Characterization of GABAergic Projection Neurons from Ventral Hippocampus to Amygdala. Brain Sci. 2015; 5:299–317. [PubMed: 26264032]

Mattis J, Brill J, Evans S, Lerner T, Davidson T, Hyun M, Ramakrishnan C, Deisseroth K, Huguenard J. Frequency-dependent, cell type-divergent signaling in the hippocamposeptal projection. The Journal of neuroscience : the official journal of the Society for Neuroscience. 2014; 34:11769–11780. [PubMed: 25164672]

Melzer S, Michael M, Caputi A, Eliava M, Fuchs EC, Whittington MA, Monyer H. Long-range-projecting GABAergic neurons modulate inhibition in hippocampus and entorhinal cortex. Science. 2012; 335:1506–1510. [PubMed: 22442486]

Peng Z, Zhang N, Wei W, Huang CS, Cetina Y, Otis TS, Houser CR. A reorganized GABAergic circuit in a model of epilepsy: evidence from optogenetic labeling and stimulation of somatostatin interneurons. J Neurosci. 2013; 33:14392–14405. [PubMed: 24005292]

Ratzliff AD, Howard AL, Santhakumar V, Osapay I, Soltesz I. Rapid deletion of mossy cells does not result in a hyperexcitable dentate gyrus: implications for epileptogenesis. J Neurosci. 2004; 24:2259–2269. [PubMed: 14999076]

Ribak CE, Seress L, Amaral DG. The development, ultrastructure and synaptic connections of the mossy cells of the dentate gyrus. J Neurocytol. 1985; 14:835–857. [PubMed: 2419523]

Ribak CE, Seress L, Peterson GM, Seroogy KB, Fallon JH, Schmued LC. A GABAergic inhibitory component within the hippocampal commissural pathway. J Neurosci. 1986; 6:3492–3498. [PubMed: 2432200]

Santhakumar V, Aradi I, Soltesz I. Role of mossy fiber sprouting and mossy cell loss in hyperexcitability: a network model of the dentate gyrus incorporating cell types and axonal topography. J Neurophysiol. 2005; 93:437–453. [PubMed: 15342722]

Scharfman HE, Pierce JP. New insights into the role of hilar ectopic granule cells in the dentate gyrus based on quantitative anatomic analysis and three-dimensional reconstruction. Epilepsia. 2012; 53 Suppl 1:109–115. [PubMed: 22612815]

Sohal VS, Zhang F, Yizhar O, Deisseroth K. Parvalbumin neurons and gamma rhythms enhance cortical circuit performance. Nature. 2009; 459:698–702. [PubMed: 19396159]

Soussi R, Boulland J-LL, Bassot E, Bras H, Coulon P, Chaudhry FA, Storm-Mathisen J, Ferhat L, Esclapez M. Reorganization of supramammillary-hippocampal pathways in the rat pilocarpine model of temporal lobe epilepsy: evidence for axon terminal sprouting. Brain Struct Funct. 2015; 220:2449–2468. [PubMed: 24889162]

Sun Y, Nguyen AQ, Nguyen JP, Le L, Saur D, Choi J, Callaway EM, Xu X. Cell-type-specific circuit connectivity of hippocampal CA1 revealed through Cre-dependent rabies tracing. Cell Rep. 2014; 7:269–280. [PubMed: 24656815]

Sutula T, Cascino G, Cavazos J, Parada I, Ramirez L. Mossy fiber synaptic reorganization in the epileptic human temporal lobe. Ann Neurol. 1989; 26:321–330. [PubMed: 2508534]

Tákacs VT, Freund TF, Gulyás AI. Types and synaptic connections of hippocampal inhibitory neurons reciprocally connected with the medial septum. Eur J Neurosci. 2008; 28:148–164. [PubMed: 18662340]

Tauck DL, Nadler JV. Evidence of functional mossy fiber sprouting in hippocampal formation of kainic acid-treated rats. J Neurosci. 1985; 5:1016–1022. [PubMed: 3981241]

Tóth K, Borhegyi Z, Freund TF. Postsynaptic targets of GABAergic hippocampal neurons in the medial septum-diagonal band of broca complex. J Neurosci Official J Soc Neurosci. 1993; 13:3712–3724.

Zappone CA, Sloviter RS. Commissurally projecting inhibitory interneurons of the rat hippocampal dentate gyrus: a colocalization study of neuronal markers and the retrograde tracer Fluoro-gold. J Comp Neurol. 2001; 441:324–344. [PubMed: 11745653]

Zhang W, Yamawaki R, Wen X, Uhl J, Diaz J, Prince DA, Buckmaster PS. Surviving hilar somatostatin interneurons enlarge, sprout axons, and form new synapses with granule cells in a mouse model of temporal lobe epilepsy. J Neurosci. 2009; 29:14247–14256. [PubMed: 19906972]

SIGNIFICANCE STATEMENT

Temporal lobe epilepsy is a debilitating disorder for many individuals, too many of whom do not experience seizure relief with currently available anti-epileptic therapies. One hallmark of temporal lobe epilepsy is reorganization of the hippocampal network. In this paper we report sprouting of long-range, commissural, inhibitory axons. Prior research indicates that PV interneurons contralateral to the presumed seizure focus can inhibit seizures; future anti-seizure therapies may be able to harness hippocampal reorganization and long-range inhibitory projections to provide seizure control.

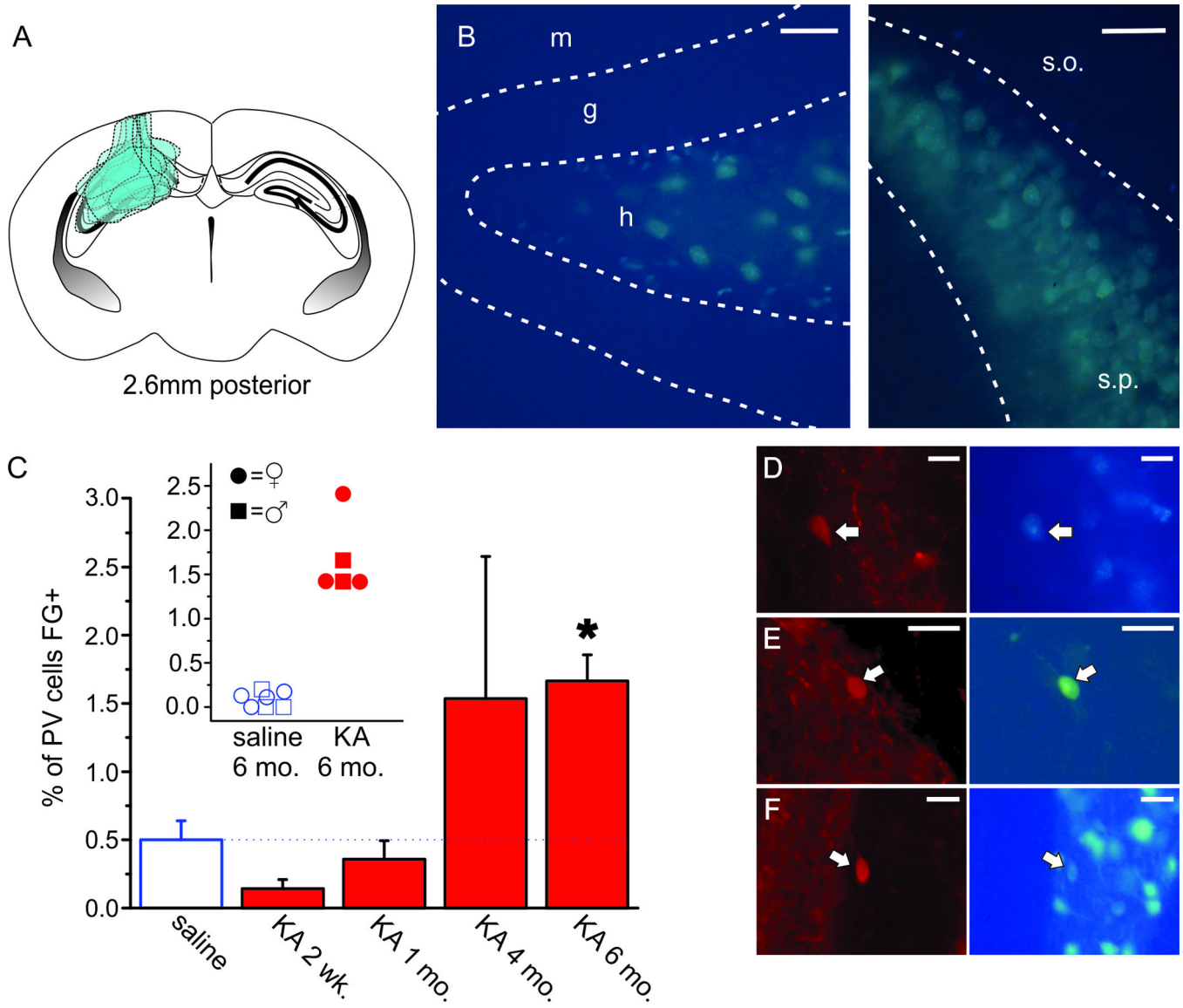

Figure 1. Parvalbumin (PV)+ interneurons retrogradely labeled with Fluorogold (FG) in the hippocampus increase by 6 months following KA injection

A) Schematic coronal section of a mouse brain at 2.6mm posterior to bregma, the site of FG injection, illustrating the extent of FG seen acutely following FG injection in 9 different mice, including injection tracts through retrosplenial cortex and hippocampus. FG was also seen in the most dorsal aspect of the thalamus in 4 of 9 mice. In all mice, FG did not invade the contralateral hippocampus. **B)** Retrograde FG labeling in dentate hilar neurons (left panel) and CA3 pyramidal layer neurons (right panel), verifying retrograde tracing. As expected, no granule cells were labeled with FG (left panel). Molecular layer (m), granular layer (g), hilus (h), stratum oriens (s.o.), stratum pyramidale (s.p.). Scale bars = 50μm (left panel), 100μm (right panel). **C)** Percent of PV+ interneurons co-labeled with FG in controls (open bar) and KA-injected animals by time post KA injection. Asterisk indicates a *p*-value of less than 0.01 (6 months post-KA vs. saline controls, Mann-Whitney test with Bonferonni correction for multiple comparisons). Inset shows the percentage of PV+ interneurons co-

labeled with FG in individual animals 6 month post-saline and 6 months post-KA. Female mice denoted by circles, male mice denoted by squares. There is no apparent sex difference. Overlapping points are offset. **D–F)** PV immunofluorescent cells (left panels) co-labeled with FG (right panels) in CA3 **(D)**, CA1 **(E)**, and the dentate gyrus (DG) **(F)** of the hippocampus contralateral to the site of kainate (KA), saline, and FG injections. Arrows indicate PV+ cells co-labeled with FG. Scale bars = 25μm (D–F).

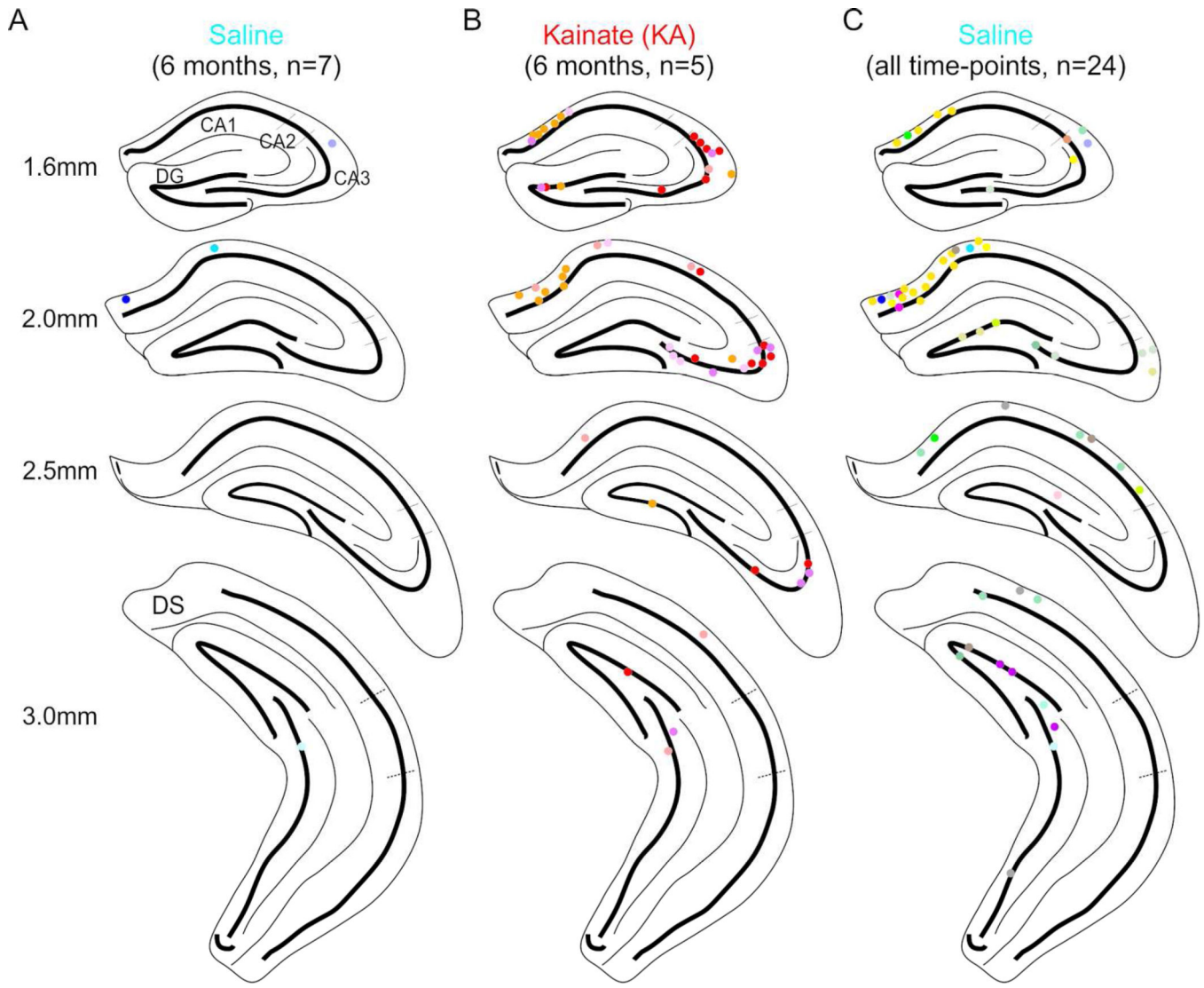

Figure 2. PV+ interneurons co-labeled with FG located throughout the hippocampus

A–B) PV+ interneurons co-labeled with FG collapsed onto a coronal view of 4 different positions posterior from bregma in saline-injected **(A)** or KA-injected **(B)** animals (n = 6 saline, 5 KA) at the 6 month time-point found in CA1, CA3, and the DG. Note the increased number of retrogradely labeled cells following KA **(B)** compared to saline **(A)**. **C)** PV+ interneurons co-labeled with FG from all saline-injected animals (n = 24). Each color represents cells from an individual mouse. Dorsal subiculum (DS).

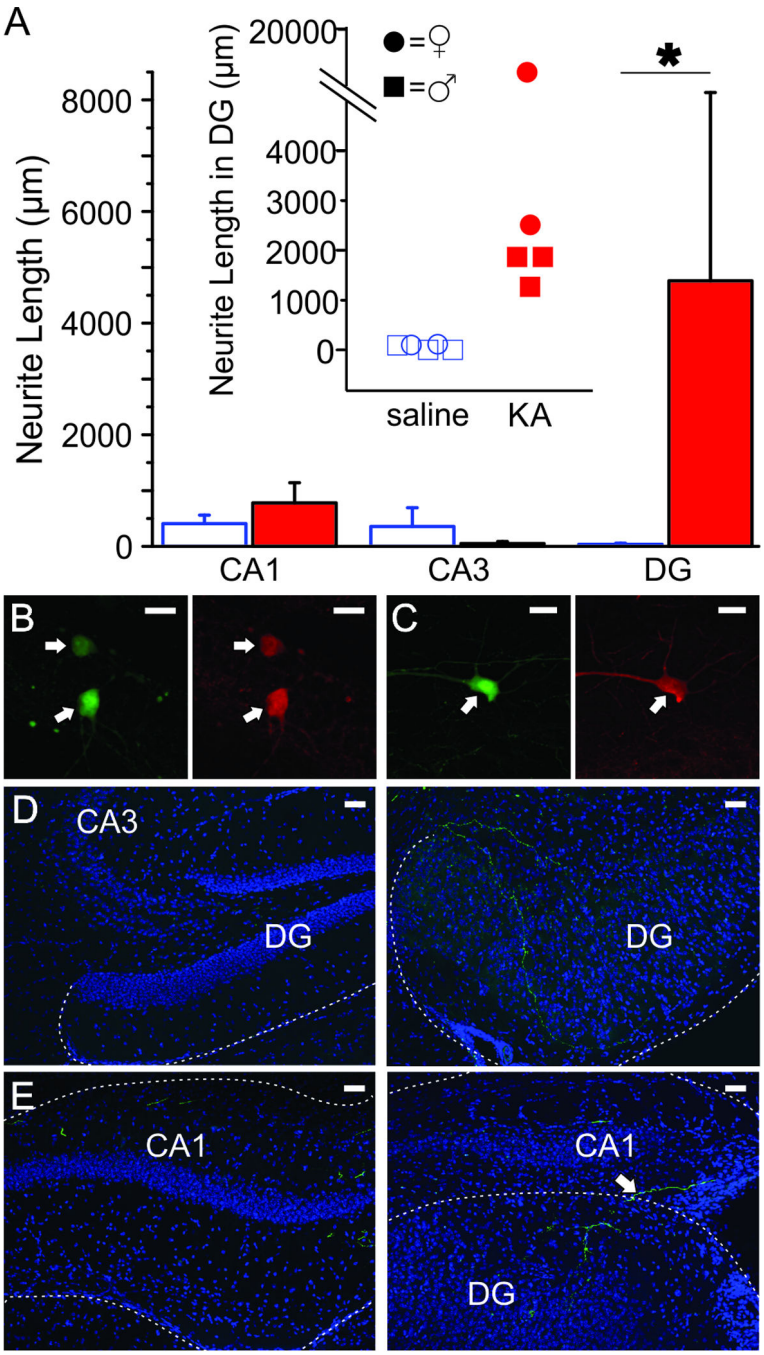

Figure 3. Commissural projections sprout in the DG 6 months following KA injection

A) Mean length of GFP-labeled fibers located in CA1, CA3, and the DG 6 months post-KA (closed, red bars) or saline (open bars) at 0.84mm left of the sagittal sinus. Asterisk indicates *p*-value of less than 0.05 (Mann-Whitney, length of neurites located in DG 6 months post-KA vs. 6 months post-saline). Inset shows the length of GFP-labeled fibers in the DG of individual mice 6 months post-KA or saline. Female mice denoted by circles, male mice denoted by squares. There is no apparent sex difference. Overlapping points are offset. **B–C)** GFP-labeled cells (left panels) in the right (virus-injected) hippocampus are confirmed PV-

immunoreactive (right panels) in DG **(B)** and CA1 **(C)**. Scale bars = 20μm. **D–E)** In the DG there is significant sprouting of commissural fibers from PV neurons (GFP-labeled fibers) six months after KA-injection (right panels) compared to after saline injection (left panels). Fibers are seen entering the DG from the CA3 region (right panel D) and by crossing the hippocampal fissure (right panel E). Granule cell dispersion is apparent in KA injected animals. Shown with DAPI in blue. Scale bar = 50μm.

Table I

Table of primary antibody used

Antigen	Description of Immunogen	Source, Host Species, Cat. #, lot #, RRID	Concentration Used
Parvalbumin	Calcium-binding albumin protein	Swant, rabbit, Cat. # PV27, lot 2014, RRID: AB_2631173	0.001ug/ul